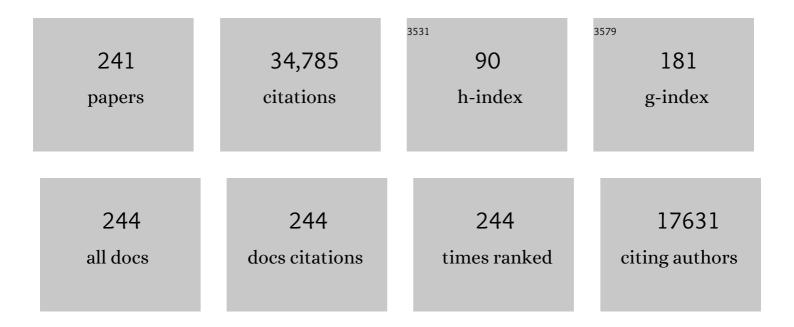
Wenxing Chen

List of Publications by Year in descending order

Source: https://exaly.com/author-pdf/2236115/publications.pdf Version: 2024-02-01



#	Article	IF	CITATIONS
1	Surface Molecular Encapsulation with Cyclodextrin in Promoting the Activity and Stability of Fe Singleâ€Atom Catalyst for Oxygen Reduction Reaction. Energy and Environmental Materials, 2023, 6, .	12.8	11
2	Construction of Synergistic Co and Cu Diatomic Sites for Enhanced Higher Alcohol Synthesis. CCS Chemistry, 2023, 5, 851-864.	7.8	4
3	Solar-driven zinc-doped graphitic carbon nitride photocatalytic fibre for simultaneous removal of hexavalent chromium and pharmaceuticals. Environmental Technology (United Kingdom), 2022, 43, 2569-2580.	2.2	6
4	Rational design of Fe-N-C electrocatalysts for oxygen reduction reaction: From nanoparticles to single atoms. Nano Research, 2022, 15, 1753-1778.	10.4	44
5	RuO2 clusters derived from bulk SrRuO3: Robust catalyst for oxygen evolution reaction in acid. Nano Research, 2022, 15, 1959-1965.	10.4	23
6	Reaction kinetics of melt postâ€polycondensation process for polycarbonate in film state. Journal of Applied Polymer Science, 2022, 139, 51731.	2.6	4
7	Interfacial engineering of 3D hollow CoSe2@ultrathin MoSe2 core@shell heterostructure for efficient pH-universal hydrogen evolution reaction. Nano Research, 2022, 15, 2895-2904.	10.4	64
8	Identification of Fenton-like active Cu sites by heteroatom modulation of electronic density. Proceedings of the National Academy of Sciences of the United States of America, 2022, 119, .	7.1	132
9	Complementary Operando Spectroscopy identification of in-situ generated metastable charge-asymmetry Cu2-CuN3 clusters for CO2 reduction to ethanol. Nature Communications, 2022, 13, 1322.	12.8	113
10	Hydrodynamics and mixing performance in a continuous miniature conical counter-rotating twin-screw extruder. International Journal of Chemical Reactor Engineering, 2022, .	1.1	3
11	Abiotic degradation behavior of polyacrylonitrile-based material filled with a composite of TiO2 and g-C3N4 under solar illumination. Chemosphere, 2022, 299, 134375.	8.2	8
12	Efficient peroxymonosulfate activation by N-rich pyridyl-iron phthalocyanine derivative for the elimination of pharmaceutical contaminants under solar irradiation. Chemosphere, 2022, 299, 134464.	8.2	2
13	Theoretical Predictions, Experimental Modulation Strategies, and Applications of MXeneâ€Supported Atomically Dispersed Metal Sites. Small, 2022, 18, e2105883.	10.0	28
14	Carbon-supported high-entropy Co-Zn-Cd-Cu-Mn sulfide nanoarrays promise high-performance overall water splitting. Nano Research, 2022, 15, 6054-6061.	10.4	47
15	Silver based single atom catalyst with heteroatom coordination environment as high performance oxygen reduction reaction catalyst. Nano Research, 2022, 15, 7968-7975.	10.4	20
16	Construction of interconnected NiO/CoFe alloy nanosheets for overall water splitting. Renewable Energy, 2022, 194, 459-468.	8.9	15
17	Research progress of asymmetrically coordinated single-atom catalysts for electrocatalytic reactions. Journal of Materials Chemistry A, 2022, 10, 14732-14746.	10.3	38
18	Degradation of carbamazepine by MWCNTs-promoted generation of high-valent iron-oxo species in a mild system with O-bridged iron perfluorophthalocyanine dimers. Journal of Environmental Sciences, 2021, 99, 260-266.	6.1	6

#	Article	IF	CITATIONS
19	Atomicâ€Level Modulation of Electronic Density at Cobalt Singleâ€Atom Sites Derived from Metal–Organic Frameworks: Enhanced Oxygen Reduction Performance. Angewandte Chemie - International Edition, 2021, 60, 3212-3221.	13.8	445
20	Atomicâ€Level Modulation of Electronic Density at Cobalt Singleâ€Atom Sites Derived from Metal–Organic Frameworks: Enhanced Oxygen Reduction Performance. Angewandte Chemie, 2021, 133, 3249-3258.	2.0	44
21	Single copper sites dispersed on hierarchically porous carbon for improving oxygen reduction reaction towards zinc-air battery. Nano Research, 2021, 14, 998-1003.	10.4	50
22	Single-atom Fe with Fe1N3 structure showing superior performances for both hydrogenation and transfer hydrogenation of nitrobenzene. Science China Materials, 2021, 64, 642-650.	6.3	98
23	A rational design of an efficient counter electrode with the Co/Co ₁ P ₁ N ₃ atomic interface for promoting catalytic performance. Materials Chemistry Frontiers, 2021, 5, 3085-3092.	5.9	8
24	Metal single-atom catalysts for selective hydrogenation of unsaturated bonds. Journal of Materials Chemistry A, 2021, 9, 5296-5319.	10.3	43
25	Bottom-up pore-generation strategy modulated active nitrogen species for oxygen reduction reaction. Materials Chemistry Frontiers, 2021, 5, 2684-2693.	5.9	4
26	Highly Active and Stable Palladium Single-Atom Catalyst Achieved by a Thermal Atomization Strategy on an SBA-15 Molecular Sieve for Semi-Hydrogenation Reactions. ACS Applied Materials & Interfaces, 2021, 13, 2530-2537.	8.0	31
27	Artificial light-harvesting 2D photosynthetic systems with iron phthalocyanine/graphitic carbon nitride composites for highly efficient CO ₂ reduction. Catalysis Science and Technology, 2021, 11, 5952-5961.	4.1	10
28	Copper-based single-atom alloys for heterogeneous catalysis. Chemical Communications, 2021, 57, 2710-2723.	4.1	22
29	Biomimetic polydopamine catalyst with redox activity for oxygen-promoted H ₂ production <i>via</i> aqueous formaldehyde reforming. Sustainable Energy and Fuels, 2021, 5, 4575-4579.	4.9	2
30	A general strategy to prepare atomically dispersed biomimetic catalysts based on host–guest chemistry. Chemical Communications, 2021, 57, 1895-1898.	4.1	2
31	Saltâ€Induced Changes in Solâ€toâ€Gel Transition and Structure of Stereocomplexable Poly(lactic) Tj ETQq1 1	0.784314 2.2	rgBT /Overloo
32	Notched-Polyoxometalate Strategy to Fabricate Atomically Dispersed Ru Catalysts for Biomass Conversion. ACS Catalysis, 2021, 11, 2669-2675.	11.2	34
33	Construction of Dualâ€Activeâ€6ite Copper Catalyst Containing both CuN ₃ and CuN ₄ Sites. Small, 2021, 17, e2006834.	10.0	52
34	Oxygen Reduction Reaction: MnN ₄ Oxygen Reduction Electrocatalyst: Operando Investigation of Active Sites and High Performance in Zinc–Air Battery (Adv. Energy Mater. 6/2021). Advanced Energy Materials, 2021, 11, 2170025.	19.5	0
35	A highly accessible copper single-atom catalyst for wound antibacterial application. Nano Research, 2021, 14, 4808-4813.	10.4	35
36	Single atom catalysts by atomic diffusion strategy. Nano Research, 2021, 14, 4398-4416.	10.4	51

#	Article	IF	CITATIONS
37	Engineering Ag–N <i>_x</i> Single-Atom Sites on Porous Concave N-Doped Carbon for Boosting CO ₂ Electroreduction. ACS Applied Materials & Interfaces, 2021, 13, 17736-17744.	8.0	45
38	Electron-rich isolated Pt active sites in ultrafine PtFe3 intermetallic catalyst for efficient alkene hydrosilylation. Journal of Catalysis, 2021, 396, 351-359.	6.2	16
39	Optimized MoP with Pseudo-Single-Atom Tungsten for Efficient Hydrogen Electrocatalysis. Chemistry of Materials, 2021, 33, 3639-3649.	6.7	20
40	Dual-atom Pt heterogeneous catalyst with excellent catalytic performances for the selective hydrogenation and epoxidation. Nature Communications, 2021, 12, 3181.	12.8	156
41	Transforming cobalt hydroxide nanowires into single atom site catalysts. Nano Energy, 2021, 83, 105799.	16.0	19
42	Matching the kinetics of natural enzymes with a single-atom iron nanozyme. Nature Catalysis, 2021, 4, 407-417.	34.4	517
43	High-valent iron-oxo species on pyridine-containing MWCNTs generated in a solar-induced H2O2 activation system for the removal of antimicrobials. Chemosphere, 2021, 273, 129545.	8.2	6
44	Ultrafast Rechargeable Aqueous Zincâ€ion Batteries Based on Stable Radical Chemistry. Advanced Functional Materials, 2021, 31, 2102011.	14.9	56
45	Cactus-like NiCo2S4@NiFe LDH hollow spheres as an effective oxygen bifunctional electrocatalyst in alkaline solution. Applied Catalysis B: Environmental, 2021, 286, 119869.	20.2	176
46	Structure and properties of gelâ€spun ultraâ€high molecular weight polyethylene fibers obtained from industrial production line. Journal of Applied Polymer Science, 2021, 138, 51317.	2.6	6
47	In Situ Implanting of Single Tungsten Sites into Defective UiOâ€66(Zr) by Solventâ€Free Route for Efficient Oxidative Desulfurization at Room Temperature. Angewandte Chemie, 2021, 133, 20481-20487.	2.0	6
48	In Situ Implanting of Single Tungsten Sites into Defective UiOâ€66(Zr) by Solventâ€Free Route for Efficient Oxidative Desulfurization at Room Temperature. Angewandte Chemie - International Edition, 2021, 60, 20318-20324.	13.8	81
49	Electrocatalytic acidic oxygen evolution reaction: From nanocrystals to single atoms. Aggregate, 2021, 2, e106.	9.9	27
50	Frontispiece: In Situ Implanting of Single Tungsten Sites into Defective UiOâ€66(Zr) by Solventâ€Free Route for Efficient Oxidative Desulfurization at Room Temperature. Angewandte Chemie - International Edition, 2021, 60, .	13.8	0
51	Frontispiz: In Situ Implanting of Single Tungsten Sites into Defective UiOâ€66(Zr) by Solventâ€Free Route for Efficient Oxidative Desulfurization at Room Temperature. Angewandte Chemie, 2021, 133, .	2.0	0
52	Atomic-Scale Tailoring and Molecular-Level Tracking of Oxygen-Containing Tungsten Single-Atom Catalysts with Enhanced Singlet Oxygen Generation. ACS Applied Materials & Interfaces, 2021, 13, 37142-37151.	8.0	9
53	Structural revolution of atomically dispersed Mn sites dictates oxygen reduction performance. Nano Research, 2021, 14, 4512-4519.	10.4	40
54	Controllable drilling by corrosive Cu1Ox to access highly accessible single-site catalysts for bacterial disinfection. Applied Catalysis B: Environmental, 2021, 293, 120228.	20.2	11

#	Article	IF	CITATIONS
55	Alkyne Semihydrogenation over Pd Nanoparticles Embedded in N,S-Doped Carbon Nanosheets. ACS Applied Nano Materials, 2021, 4, 9052-9059.	5.0	6
56	Atomically dispersed Ru in Pt ₃ Sn intermetallic alloy as an efficient methanol oxidation electrocatalyst. Chemical Communications, 2021, 57, 2164-2167.	4.1	14
57	Atomic regulation of metal–organic framework derived carbon-based single-atom catalysts for the electrochemical CO ₂ reduction reaction. Journal of Materials Chemistry A, 2021, 9, 23382-23418.	10.3	46
58	Simultaneous diffusion of cation and anion to access N, S co-coordinated Bi-sites for enhanced CO2 electroreduction. Nano Research, 2021, 14, 2790-2796.	10.4	53
59	Integrating single-cobalt-site and electric field of boron nitride in dechlorination electrocatalysts by bioinspired design. Nature Communications, 2021, 12, 303.	12.8	97
60	Simultaneous oxidative and reductive reactions in one system by atomic design. Nature Catalysis, 2021, 4, 134-143.	34.4	132
61	N-Bridged Co–N–Ni: new bimetallic sites for promoting electrochemical CO ₂ reduction. Energy and Environmental Science, 2021, 14, 3019-3028.	30.8	128
62	MnN ₄ Oxygen Reduction Electrocatalyst: Operando Investigation of Active Sites and High Performance in Zinc–Air Battery. Advanced Energy Materials, 2021, 11, 2002753.	19.5	83
63	Atomically dispersed Pd catalysts promote the oxygen evolution reaction in acidic media. Chemical Communications, 2021, 57, 11561-11564.	4.1	10
64	Factors Influencing the Performance of Copper-Bearing Catalysts in the CO ₂ Reduction System. ACS Energy Letters, 2021, 6, 3992-4022.	17.4	58
65	A single-atom Cu–N ₂ catalyst eliminates oxygen interference for electrochemical sensing of hydrogen peroxide in a living animal brain. Chemical Science, 2021, 12, 15045-15053.	7.4	36
66	Flexible Electron-Rich Ion Channels Enable Ultrafast and Stable Aqueous Zinc-Ion Storage. ACS Applied Materials & Interfaces, 2021, 13, 54096-54105.	8.0	10
67	Single-Atom Ru on Al ₂ O ₃ for Highly Active and Selective 1,2-Dichloroethane Catalytic Degradation. ACS Applied Materials & Interfaces, 2021, 13, 53683-53690.	8.0	16
68	Phase and interface engineering of nickel carbide nanobranches for efficient hydrogen oxidation catalysis. Journal of Materials Chemistry A, 2021, 9, 26323-26329.	10.3	12
69	Engineering the Atomic Interface with Single Platinum Atoms for Enhanced Photocatalytic Hydrogen Production. Angewandte Chemie, 2020, 132, 1311-1317.	2.0	59
70	Engineering the Atomic Interface with Single Platinum Atoms for Enhanced Photocatalytic Hydrogen Production. Angewandte Chemie - International Edition, 2020, 59, 1295-1301.	13.8	344
71	Atomically dispersed Fe atoms anchored on COF-derived N-doped carbon nanospheres as efficient multi-functional catalysts. Chemical Science, 2020, 11, 786-790.	7.4	110
72	Single iron atoms coordinated to g-C ₃ N ₄ on hierarchical porous N-doped carbon polyhedra as a high-performance electrocatalyst for the oxygen reduction reaction. Chemical Communications, 2020, 56, 798-801.	4.1	45

#	Article	IF	CITATIONS
73	Construction of MnO ₂ Artificial Leaf with Atomic Thickness as Highly Stable Battery Anodes. Advanced Materials, 2020, 32, e1906582.	21.0	57
74	High-Valent Iron-Oxo Complexes as Dominant Species to Eliminate Pharmaceuticals and Chloride-Containing Intermediates by the Activation of Peroxymonosulfate Under Visible Irradiation. Catalysis Letters, 2020, 150, 1355-1367.	2.6	11
75	Single-atom Sn-Zn pairs in CuO catalyst promote dimethyldichlorosilane synthesis. National Science Review, 2020, 7, 600-608.	9.5	42
76	Confined crystallization and melting behaviors of poly(ethylene glycol) endâ€functionalized by hydrogen bonding groups: Effect of contents for functional units. Polymer Crystallization, 2020, 3, e10158.	0.8	3
77	Dynamic evolution of isolated Ru–FeP atomic interface sites for promoting the electrochemical hydrogen evolution reaction. Journal of Materials Chemistry A, 2020, 8, 22607-22612.	10.3	36
78	Controlling N-doping type in carbon to boost single-atom site Cu catalyzed transfer hydrogenation of quinoline. Nano Research, 2020, 13, 3082-3087.	10.4	215
79	Engineering of Coordination Environment and Multiscale Structure in Single-Site Copper Catalyst for Superior Electrocatalytic Oxygen Reduction. Nano Letters, 2020, 20, 6206-6214.	9.1	178
80	Discovery of main group single Sb–N ₄ active sites for CO ₂ electroreduction to formate with high efficiency. Energy and Environmental Science, 2020, 13, 2856-2863.	30.8	245
81	Gramâ€5cale Synthesis of Highâ€Loading Singleâ€Atomicâ€5ite Fe Catalysts for Effective Epoxidation of Styrene. Advanced Materials, 2020, 32, e2000896.	21.0	181
82	Direct Synthesis of Atomically Dispersed Palladium Atoms Supported on Graphitic Carbon Nitride for Efficient Selective Hydrogenation Reactions. ACS Applied Materials & Interfaces, 2020, 12, 54146-54154.	8.0	31
83	Negative Pressure Pyrolysis Induced Highly Accessible Single Sites Dispersed on 3D Graphene Frameworks for Enhanced Oxygen Reduction. Angewandte Chemie, 2020, 132, 20645-20649.	2.0	16
84	Negative Pressure Pyrolysis Induced Highly Accessible Single Sites Dispersed on 3D Graphene Frameworks for Enhanced Oxygen Reduction. Angewandte Chemie - International Edition, 2020, 59, 20465-20469.	13.8	104
85	Design of a Singleâ€Atom Indium ^{Î′+} –N ₄ Interface for Efficient Electroreduction of CO ₂ to Formate. Angewandte Chemie - International Edition, 2020, 59, 22465-22469.	13.8	232
86	Design of a Singleâ€Atom Indium δ+ –N 4 Interface for Efficient Electroreduction of CO 2 to Formate. Angewandte Chemie, 2020, 132, 22651-22655.	2.0	29
87	Unique Cation Exchange in Nanocrystal Matrix via Surface Vacancy Engineering Overcoming Chemical Kinetic Energy Barriers. CheM, 2020, 6, 3086-3099.	11.7	18
88	Single-Atom Co–N ₄ Electrocatalyst Enabling Four-Electron Oxygen Reduction with Enhanced Hydrogen Peroxide Tolerance for Selective Sensing. Journal of the American Chemical Society, 2020, 142, 16861-16867.	13.7	184
89	Crystallization and Thermal Behaviors of Poly(ethylene terephthalate)/Bisphenols Complexes through Melt Post-Polycondensation. Polymers, 2020, 12, 3053.	4.5	13
90	Selective Hydrogenation on a Highly Active Single-Atom Catalyst of Palladium Dispersed on Ceria Nanorods by Defect Engineering. ACS Applied Materials & Interfaces, 2020, 12, 57569-57577.	8.0	34

#	Article	IF	CITATIONS
91	Fabrication of a wrinkled structure made of wearable polyacrylonitrile/polyurethane composite fibers with elastic sensing properties suitable for human movement detection. Polymer Composites, 2020, 41, 3491-3500.	4.6	6
92	Coordination structure dominated performance of single-atomic Pt catalyst for anti-Markovnikov hydroboration of alkenes. Science China Materials, 2020, 63, 972-981.	6.3	74
93	Engineering a metal–organic framework derived Mn–N ₄ –C _x S _y atomic interface for highly efficient oxygen reduction reaction. Chemical Science, 2020, 11, 5994-5999.	7.4	113
94	Room-Temperature Synthesis of Single Iron Site by Electrofiltration for Photoreduction of CO ₂ into Tunable Syngas. ACS Nano, 2020, 14, 6164-6172.	14.6	71
95	Iridium single-atom catalyst on nitrogen-doped carbon for formic acid oxidation synthesized using a general host–guest strategy. Nature Chemistry, 2020, 12, 764-772.	13.6	452
96	Engineering unsymmetrically coordinated Cu-S1N3 single atom sites with enhanced oxygen reduction activity. Nature Communications, 2020, 11, 3049.	12.8	537
97	Single-atom Ni-N4 provides a robust cellular NO sensor. Nature Communications, 2020, 11, 3188.	12.8	153
98	Engineering Isolated Mn–N ₂ C ₂ Atomic Interface Sites for Efficient Bifunctional Oxygen Reduction and Evolution Reaction. Nano Letters, 2020, 20, 5443-5450.	9.1	249
99	Fabricating Pd isolated single atom sites on C3N4/rGO for heterogenization of homogeneous catalysis. Nano Research, 2020, 13, 947-951.	10.4	65
100	Single-atom Rh/N-doped carbon electrocatalyst for formic acid oxidation. Nature Nanotechnology, 2020, 15, 390-397.	31.5	420
101	Cation/Anion Exchange Reactions toward the Syntheses of Upgraded Nanostructures: Principles and Applications. Matter, 2020, 2, 554-586.	10.0	81
102	In-situ polymerization induced atomically dispersed manganese sites as cocatalyst for CO2 photoreduction into synthesis gas. Nano Energy, 2020, 76, 105059.	16.0	60
103	Single-Atom Au ^I –N ₃ Site for Acetylene Hydrochlorination Reaction. ACS Catalysis, 2020, 10, 1865-1870.	11.2	76
104	Tuning Polarity of Cu-O Bond in Heterogeneous Cu Catalyst to Promote Additive-free Hydroboration of Alkynes. CheM, 2020, 6, 725-737.	11.7	87
105	Confined crystallization, melting behavior and morphology in PEGâ€ <i>b</i> â€PLA diblock copolymers: Amorphous versus crystalline PLA. Journal of Polymer Science, 2020, 58, 455-465.	3.8	13
106	Film reaction kinetics for melt postpolycondensation of poly(ethylene terephthalate). Journal of Applied Polymer Science, 2020, 137, 48988.	2.6	6
107	Atomic-dispersed platinum anchored on porous alumina sheets as an efficient catalyst for diboration of alkynes. Chemical Communications, 2020, 56, 3127-3130.	4.1	17
108	Highly Selective Photoreduction of CO ₂ with Suppressing H ₂ Evolution by Plasmonic Au/CdSe–Cu ₂ O Hierarchical Nanostructures under Visible Light. Small, 2020, 16, e2000426.	10.0	53

#	Article	IF	CITATIONS
109	Micro-scale 2D quasi-nanosheets formed by 0D nanocrystals: from single to multicomponent building blocks. Science China Materials, 2020, 63, 1265-1271.	6.3	10
110	Promoting electrocatalytic methanol oxidation of platinum nanoparticles by cerium modification. Nano Energy, 2020, 73, 104784.	16.0	54
111	Isolated Ni Atoms Dispersed on Ru Nanosheets: High-Performance Electrocatalysts toward Hydrogen Oxidation Reaction. Nano Letters, 2020, 20, 3442-3448.	9.1	172
112	In Situ Phosphatizing of Triphenylphosphine Encapsulated within Metal–Organic Frameworks to Design Atomic Co ₁ –P ₁ N ₃ Interfacial Structure for Promoting Catalytic Performance. Journal of the American Chemical Society, 2020, 142, 8431-8439.	13.7	259
113	Electrochemical conversion of bulk platinum into platinum single-atom sites for the hydrogen evolution reaction. Journal of Materials Chemistry A, 2020, 8, 10755-10760.	10.3	40
114	Directly transforming copper (I) oxide bulk into isolated single-atom copper sites catalyst through gas-transport approach. Nature Communications, 2019, 10, 3734.	12.8	276
115	Edge-Contact Geometry and Anion-Deficit Construction for Activating Ultrathin MoS ₂ on W ₁₇ O ₄₇ in the Hydrogen Evolution Reaction. Inorganic Chemistry, 2019, 58, 11241-11247.	4.0	10
116	Revealing the role of graphene in enhancing the catalytic performance of phthalocyanine immobilized graphene/bacterial cellulose nanocomposite. Cellulose, 2019, 26, 7863-7875.	4.9	6
117	Isolating contiguous Pt atoms and forming Pt-Zn intermetallic nanoparticles to regulate selectivity in 4-nitrophenylacetylene hydrogenation. Nature Communications, 2019, 10, 3787.	12.8	119
118	Evolution of Hollow CuInS ₂ Nanododecahedrons via Kirkendall Effect Driven by Cation Exchange for Efficient Solar Water Splitting. ACS Applied Materials & Interfaces, 2019, 11, 27170-27177.	8.0	40
119	Mesoporous Nitrogenâ€Doped Carbonâ€Nanosphereâ€Supported Isolated Singleâ€Atom Pd Catalyst for Highly Efficient Semihydrogenation of Acetylene. Advanced Materials, 2019, 31, e1901024.	21.0	146
120	Bismuth Single Atoms Resulting from Transformation of Metal–Organic Frameworks and Their Use as Electrocatalysts for CO ₂ Reduction. Journal of the American Chemical Society, 2019, 141, 16569-16573.	13.7	501
121	Silkâ€Derived 2D Porous Carbon Nanosheets with Atomicallyâ€Dispersed Feâ€N <i>_x</i> Sites for Highly Efficient Oxygen Reaction Catalysts. Small, 2019, 15, e1804966.	10.0	64
122	Boosting Oxygen Reduction Catalysis with Fe–N ₄ Sites Decorated Porous Carbons toward Fuel Cells. ACS Catalysis, 2019, 9, 2158-2163.	11.2	297
123	A single-atom Fe–N ₄ catalytic site mimicking bifunctional antioxidative enzymes for oxidative stress cytoprotection. Chemical Communications, 2019, 55, 159-162.	4.1	209
124	Interpenetrating‣yncretic Microâ€Nano Hierarchy Fibers for Effective Fine Particle Capture. Advanced Engineering Materials, 2019, 21, 1801361.	3.5	3
125	Two-Step Carbothermal Welding To Access Atomically Dispersed Pd ₁ on Three-Dimensional Zirconia Nanonet for Direct Indole Synthesis. Journal of the American Chemical Society, 2019, 141, 10590-10594.	13.7	108
126	Colored TiO2 composites embedded on fabrics as photocatalysts: Decontamination of formaldehyde and deactivation of bacteria in water and air. Chemical Engineering Journal, 2019, 375, 121949.	12.7	26

#	Article	IF	CITATIONS
127	Electrodeposition of polypyrrole on He plasma etched carbon nanotube films for electrodes of flexible all-solid-state supercapacitor. Journal of Solid State Electrochemistry, 2019, 23, 1553-1562.	2.5	12
128	High-Concentration Single Atomic Pt Sites on Hollow CuSx for Selective O2 Reduction to H2O2 in Acid Solution. CheM, 2019, 5, 2099-2110.	11.7	279
129	Single-atom tailoring of platinum nanocatalysts for high-performance multifunctional electrocatalysis. Nature Catalysis, 2019, 2, 495-503.	34.4	464
130	High-Performance Quantum Dots with Synergistic Doping and Oxide Shell Protection Synthesized by Cation Exchange Conversion of Ternary-Composition Nanoparticles. Journal of Physical Chemistry Letters, 2019, 10, 2606-2615.	4.6	17
131	Regulating the Catalytic Performance of Single-Atomic-Site Ir Catalyst for Biomass Conversion by Metal–Support Interactions. ACS Catalysis, 2019, 9, 5223-5230.	11.2	87
132	A general route <i>via</i> formamide condensation to prepare atomically dispersed metal–nitrogen–carbon electrocatalysts for energy technologies. Energy and Environmental Science, 2019, 12, 1317-1325.	30.8	290
133	Compressive surface strained atomic-layer Cu2O on Cu@Ag nanoparticles. Nano Research, 2019, 12, 1187-1192.	10.4	21
134	Hollow anisotropic semiconductor nanoprisms with highly crystalline frameworks for high-efficiency photoelectrochemical water splitting. Journal of Materials Chemistry A, 2019, 7, 8061-8072.	10.3	16
135	Engineering the electronic structure of single atom Ru sites via compressive strain boosts acidic water oxidation electrocatalysis. Nature Catalysis, 2019, 2, 304-313.	34.4	757
136	2D MOF induced accessible and exclusive Co single sites for an efficient <i>O</i> -silylation of alcohols with silanes. Chemical Communications, 2019, 55, 6563-6566.	4.1	34
137	Efficient Plasmonic Au/CdSe Nanodumbbell for Photoelectrochemical Hydrogen Generation beyond Visible Region. Advanced Energy Materials, 2019, 9, 1803889.	19.5	85
138	Atomically Dispersed Ruthenium Species Inside Metal–Organic Frameworks: Combining the High Activity of Atomic Sites and the Molecular Sieving Effect of MOFs. Angewandte Chemie - International Edition, 2019, 58, 4271-4275.	13.8	162
139	Atomically Dispersed Ruthenium Species Inside Metal–Organic Frameworks: Combining the High Activity of Atomic Sites and the Molecular Sieving Effect of MOFs. Angewandte Chemie, 2019, 131, 4315-4319.	2.0	25
140	A general synthesis approach for amorphous noble metal nanosheets. Nature Communications, 2019, 10, 4855.	12.8	321
141	Two-dimensional CdX (X = Se, Te) nanosheets: controlled synthesis and their photoluminescence properties. Journal of Materials Chemistry C, 2019, 7, 13849-13858.	5.5	3
142	Atomic interface effect of a single atom copper catalyst for enhanced oxygen reduction reactions. Energy and Environmental Science, 2019, 12, 3508-3514.	30.8	278
143	Regulating the coordination environment of Co single atoms for achieving efficient electrocatalytic activity in CO2 reduction. Applied Catalysis B: Environmental, 2019, 240, 234-240.	20.2	224
144	Semiconductor Nanocrystal Engineering by Applying Thiol―and Solventâ€Coordinated Cation Exchange Kinetics. Angewandte Chemie - International Edition, 2019, 58, 4852-4857.	13.8	29

#	Article	IF	CITATIONS
145	Semiconductor Nanocrystal Engineering by Applying Thiol―and Solventâ€Coordinated Cation Exchange Kinetics. Angewandte Chemie, 2019, 131, 4906-4911.	2.0	8
146	Structure–Property Evolution of Poly(ethylene terephthalate) Fibers in Industrialized Process under Complex Coupling of Stress and Temperature Field. Macromolecules, 2019, 52, 565-574.	4.8	34
147	Continuous postâ€polycondensation of highâ€viscosity poly(ethylene terephthalate) in the molten state. Journal of Applied Polymer Science, 2019, 136, 47484.	2.6	6
148	Au@HgxCd1-xTe core@shell nanorods by sequential aqueous cation exchange for near-infrared photodetectors. Nano Energy, 2019, 57, 57-65.	16.0	38
149	Solid-Diffusion Synthesis of Single-Atom Catalysts Directly from Bulk Metal for Efficient CO2 Reduction. Joule, 2019, 3, 584-594.	24.0	277
150	Revealing the Active Species for Aerobic Alcohol Oxidation by Using Uniform Supported Palladium Catalysts. Angewandte Chemie - International Edition, 2018, 57, 4642-4646.	13.8	93
151	A Polymer Encapsulation Strategy to Synthesize Porous Nitrogenâ€Doped Carbonâ€Nanosphereâ€Supported Metal Isolatedâ€Singleâ€Atomicâ€Site Catalysts. Advanced Materials, 2018, 30, e1706508.	21.0	266
152	Design of Single-Atom Co–N ₅ Catalytic Site: A Robust Electrocatalyst for CO ₂ Reduction with Nearly 100% CO Selectivity and Remarkable Stability. Journal of the American Chemical Society, 2018, 140, 4218-4221.	13.7	945
153	Revealing the Active Species for Aerobic Alcohol Oxidation by Using Uniform Supported Palladium Catalysts. Angewandte Chemie, 2018, 130, 4732-4736.	2.0	29
154	Cation vacancy stabilization of single-atomic-site Pt1/Ni(OH)x catalyst for diboration of alkynes and alkenes. Nature Communications, 2018, 9, 1002.	12.8	255
155	PtAl truncated octahedron nanocrystals for improved formic acid electrooxidation. Chemical Communications, 2018, 54, 3951-3954.	4.1	12
156	Tuning defects in oxides at roomÂtemperature by lithium reduction. Nature Communications, 2018, 9, 1302.	12.8	428
157	Sub-nm ruthenium cluster as an efficient and robust catalyst for decomposition and synthesis of ammonia: Break the "size shackles― Nano Research, 2018, 11, 4774-4785.	10.4	49
158	Effect of Protective Agents upon the Catalytic Property of Platinum Nanocrystals. ChemCatChem, 2018, 10, 2433-2441.	3.7	12
159	Defect Effects on TiO ₂ Nanosheets: Stabilizing Single Atomic Site Au and Promoting Catalytic Properties. Advanced Materials, 2018, 30, 1705369.	21.0	751
160	Regulation of Coordination Number over Single Co Sites: Triggering the Efficient Electroreduction of CO ₂ . Angewandte Chemie - International Edition, 2018, 57, 1944-1948.	13.8	888
161	Regulation of Coordination Number over Single Co Sites: Triggering the Efficient Electroreduction of CO ₂ . Angewandte Chemie, 2018, 130, 1962-1966.	2.0	244
162	General synthesis and definitive structural identification of MN4C4 single-atom catalysts with tunable electrocatalytic activities. Nature Catalysis, 2018, 1, 63-72.	34.4	1,476

#	Article	IF	CITATIONS
163	Fe Isolated Single Atoms on S, N Codoped Carbon by Copolymer Pyrolysis Strategy for Highly Efficient Oxygen Reduction Reaction. Advanced Materials, 2018, 30, e1800588.	21.0	511
164	Isolated Fe and Co dual active sites on nitrogen-doped carbon for a highly efficient oxygen reduction reaction. Chemical Communications, 2018, 54, 4274-4277.	4.1	166
165	Singleâ€Site Au ^I Catalyst for Silane Oxidation with Water. Advanced Materials, 2018, 30, 1704720.	21.0	112
166	Catalytic degradation of sulfaquinoxalinum by polyester/poly-4-vinylpyridine nanofibers-supported iron phthalocyanine. Environmental Science and Pollution Research, 2018, 25, 5902-5910.	5.3	2
167	Accelerating water dissociation kinetics by isolating cobalt atoms into ruthenium lattice. Nature Communications, 2018, 9, 4958.	12.8	264
168	Enhanced oxygen reduction with single-atomic-site iron catalysts for a zinc-air battery and hydrogen-air fuel cell. Nature Communications, 2018, 9, 5422.	12.8	696
169	Porous platinum–silver bimetallic alloys: surface composition and strain tunability toward enhanced electrocatalysis. Nanoscale, 2018, 10, 21703-21711.	5.6	20
170	Single-atomic cobalt sites embedded in hierarchically ordered porous nitrogen-doped carbon as a superior bifunctional electrocatalyst. Proceedings of the National Academy of Sciences of the United States of America, 2018, 115, 12692-12697.	7.1	325
171	Direct transformation of bulk copper into copper single sites via emitting and trapping of atoms. Nature Catalysis, 2018, 1, 781-786.	34.4	746
172	A cocoon silk chemistry strategy to ultrathin N-doped carbon nanosheet with metal single-site catalysts. Nature Communications, 2018, 9, 3861.	12.8	210
173	Mesoporous S doped Fe–N–C materials as highly active oxygen reduction reaction catalyst. Chemical Communications, 2018, 54, 12073-12076.	4.1	44
174	Nearâ€Infrared Luminescent Ternary Ag ₃ SbS ₃ Quantum Dots by in situ Conversion of Ag Nanocrystals with Sb(C ₉ H ₁₉ COOS) ₃ . Chemistry - A European Journal, 2018, 24, 18643-18647.	3.3	5
175	One-Pot Pyrolysis to N-Doped Graphene with High-Density Pt Single Atomic Sites as Heterogeneous Catalyst for Alkene Hydrosilylation. ACS Catalysis, 2018, 8, 10004-10011.	11.2	121
176	Inâ€Situ Thermal Atomization To Convert Supported Nickel Nanoparticles into Surfaceâ€Bound Nickel Singleâ€Atom Catalysts. Angewandte Chemie - International Edition, 2018, 57, 14095-14100.	13.8	310
177	Inâ€Situ Thermal Atomization To Convert Supported Nickel Nanoparticles into Surfaceâ€Bound Nickel Singleâ€Atom Catalysts. Angewandte Chemie, 2018, 130, 14291-14296.	2.0	41
178	Temperature-Controlled Selectivity of Hydrogenation and Hydrodeoxygenation in the Conversion of Biomass Molecule by the Ru ₁ /mpg-C ₃ N ₄ Catalyst. Journal of the American Chemical Society, 2018, 140, 11161-11164.	13.7	199
179	Ordered Porous Nitrogenâ€Doped Carbon Matrix with Atomically Dispersed Cobalt Sites as an Efficient Catalyst for Dehydrogenation and Transfer Hydrogenation of Nâ€Heterocycles. Angewandte Chemie, 2018, 130, 11432-11436.	2.0	24
180	Ordered Porous Nitrogenâ€Doped Carbon Matrix with Atomically Dispersed Cobalt Sites as an Efficient Catalyst for Dehydrogenation and Transfer Hydrogenation of Nâ€Heterocycles. Angewandte Chemie - International Edition, 2018, 57, 11262-11266.	13.8	165

#	Article	IF	CITATIONS
181	MOF onfined Subâ€2 nm Atomically Ordered Intermetallic PdZn Nanoparticles as Highâ€Performance Catalysts for Selective Hydrogenation of Acetylene. Advanced Materials, 2018, 30, e1801878.	21.0	133
182	Electronic structure engineering to boost oxygen reduction activity by controlling the coordination of the central metal. Energy and Environmental Science, 2018, 11, 2348-2352.	30.8	336
183	Porphyrin-like Fe-N4 sites with sulfur adjustment on hierarchical porous carbon for different rate-determining steps in oxygen reduction reaction. Nano Research, 2018, 11, 6260-6269.	10.4	118
184	Scaleâ€Up Biomass Pathway to Cobalt Single‣ite Catalysts Anchored on Nâ€Doped Porous Carbon Nanobelt with Ultrahigh Surface Area. Advanced Functional Materials, 2018, 28, 1802167.	14.9	112
185	Direct observation of noble metal nanoparticles transforming to thermally stable single atoms. Nature Nanotechnology, 2018, 13, 856-861.	31.5	741
186	From Indiumâ€Doped Ag ₂ S to AgInS ₂ Nanocrystals: Lowâ€Temperature In Situ Conversion of Colloidal Ag ₂ S Nanoparticles and Their NIR Fluorescence. Chemistry - A European Journal, 2018, 24, 13676-13680.	3.3	20
187	Atomically dispersed Au1 catalyst towards efficient electrochemical synthesis of ammonia. Science Bulletin, 2018, 63, 1246-1253.	9.0	225
188	Phosphine ligand-mediated kinetics manipulation of aqueous cation exchange: a case study on the synthesis of Au@SnS _x core–shell nanocrystals for photoelectrochemical water splitting. Chemical Communications, 2018, 54, 9993-9996.	4.1	19
189	Discovering Partially Charged Single-Atom Pt for Enhanced Anti-Markovnikov Alkene Hydrosilylation. Journal of the American Chemical Society, 2018, 140, 7407-7410.	13.7	218
190	Carbon nitride supported Fe2 cluster catalysts with superior performance for alkene epoxidation. Nature Communications, 2018, 9, 2353.	12.8	278
191	Efficient and Robust Hydrogen Evolution: Phosphorus Nitride Imide Nanotubes as Supports for Anchoring Single Ruthenium Sites. Angewandte Chemie, 2018, 130, 9639-9644.	2.0	31
192	Single Tungsten Atoms Supported on MOFâ€Derived Nâ€Doped Carbon for Robust Electrochemical Hydrogen Evolution. Advanced Materials, 2018, 30, e1800396.	21.0	427
193	Efficient and Robust Hydrogen Evolution: Phosphorus Nitride Imide Nanotubes as Supports for Anchoring Single Ruthenium Sites. Angewandte Chemie - International Edition, 2018, 57, 9495-9500.	13.8	205
194	Synergistic effects of silica nanoparticles and reactive compatibilizer on the compatibilization of polystyrene/polyamide 6 blends. Polymer Engineering and Science, 2017, 57, 1301-1310.	3.1	13
195	Hydroxyl Radical-Dominated Catalytic Oxidation in Neutral Condition by Axially Coordinated Iron Phthalocyanine on Mercapto-Functionalized Carbon Nanotubes. Industrial & Engineering Chemistry Research, 2017, 56, 2899-2907.	3.7	14
196	Isolated Single Iron Atoms Anchored on Nâ€Doped Porous Carbon as an Efficient Electrocatalyst for the Oxygen Reduction Reaction. Angewandte Chemie - International Edition, 2017, 56, 6937-6941.	13.8	1,542
197	Isolated Single Iron Atoms Anchored on Nâ€Đoped Porous Carbon as an Efficient Electrocatalyst for the Oxygen Reduction Reaction. Angewandte Chemie, 2017, 129, 7041-7045.	2.0	306
198	Isolated Single-Atom Pd Sites in Intermetallic Nanostructures: High Catalytic Selectivity for Semihydrogenation of Alkynes. Journal of the American Chemical Society, 2017, 139, 7294-7301.	13.7	354

#	Article	IF	CITATIONS
199	Innenrücktitelbild: Isolated Single Iron Atoms Anchored on Nâ€Doped Porous Carbon as an Efficient Electrocatalyst for the Oxygen Reduction Reaction (Angew. Chem. 24/2017). Angewandte Chemie, 2017, 129, 7107-7107.	2.0	6
200	lonic Exchange of Metal–Organic Frameworks to Access Single Nickel Sites for Efficient Electroreduction of CO ₂ . Journal of the American Chemical Society, 2017, 139, 8078-8081.	13.7	1,115
201	Hierarchical Fe-doped NiO x nanotubes assembled from ultrathin nanosheets containing trivalent nickel for oxygen evolution reaction. Nano Energy, 2017, 38, 167-174.	16.0	160
202	Rational Design of Single Molybdenum Atoms Anchored on Nâ€Doped Carbon for Effective Hydrogen Evolution Reaction. Angewandte Chemie - International Edition, 2017, 56, 16086-16090.	13.8	431
203	Rational Design of Single Molybdenum Atoms Anchored on Nâ€Doped Carbon for Effective Hydrogen Evolution Reaction. Angewandte Chemie, 2017, 129, 16302-16306.	2.0	82
204	Facile synthesis of CoNi _x nanoparticles embedded in nitrogen–carbon frameworks for highly efficient electrocatalytic oxygen evolution. Chemical Communications, 2017, 53, 12177-12180.	4.1	20
205	Bimetallic Ru–Co Clusters Derived from a Confined Alloying Process within Zeolite–Imidazolate Frameworks for Efficient NH ₃ Decomposition and Synthesis. ACS Applied Materials & Interfaces, 2017, 9, 39450-39455.	8.0	51
206	Atomically Dispersed Copper–Platinum Dual Sites Alloyed with Palladium Nanorings Catalyze the Hydrogen Evolution Reaction. Angewandte Chemie, 2017, 129, 16263-16267.	2.0	53
207	Atomically Dispersed Copper–Platinum Dual Sites Alloyed with Palladium Nanorings Catalyze the Hydrogen Evolution Reaction. Angewandte Chemie - International Edition, 2017, 56, 16047-16051.	13.8	231
208	Design of ultrathin Pt-Mo-Ni nanowire catalysts for ethanol electrooxidation. Science Advances, 2017, 3, e1603068.	10.3	224
209	Hydrodeoxygenation of water-insoluble bio-oil to alkanes using a highly dispersed Pd–Mo catalyst. Nature Communications, 2017, 8, 591.	12.8	110
210	Generation of reactive cobalt oxo oxamate radical species for biomimetic oxidation of contaminants. RSC Advances, 2017, 7, 42875-42883.	3.6	3
211	Free Channel Formation around Graphitic Carbon Nitride Embedded in Porous Polyethylene Terephthalate Nanofibers with Excellent Reusability for Eliminating Antibiotics under Solar Irradiation. Industrial & Engineering Chemistry Research, 2017, 56, 11151-11160.	3.7	21
212	Rational Control of the Selectivity of a Ruthenium Catalyst for Hydrogenation of 4â€Nitrostyrene by Strain Regulation. Angewandte Chemie, 2017, 129, 12133-12137.	2.0	12
213	Rational Control of the Selectivity of a Ruthenium Catalyst for Hydrogenation of 4â€Nitrostyrene by Strain Regulation. Angewandte Chemie - International Edition, 2017, 56, 11971-11975.	13.8	93
214	Metal (Hydr)oxides@Polymer Core–Shell Strategy to Metal Single-Atom Materials. Journal of the American Chemical Society, 2017, 139, 10976-10979.	13.7	257
215	Design of N-Coordinated Dual-Metal Sites: A Stable and Active Pt-Free Catalyst for Acidic Oxygen Reduction Reaction. Journal of the American Chemical Society, 2017, 139, 17281-17284.	13.7	1,220
216	Hollow N-Doped Carbon Spheres with Isolated Cobalt Single Atomic Sites: Superior Electrocatalysts for Oxygen Reduction. Journal of the American Chemical Society, 2017, 139, 17269-17272.	13.7	556

#	Article	IF	CITATIONS
217	Confined Pyrolysis within Metal–Organic Frameworks To Form Uniform Ru ₃ Clusters for Efficient Oxidation of Alcohols. Journal of the American Chemical Society, 2017, 139, 9795-9798.	13.7	258
218	Uncoordinated Amine Groups of Metal–Organic Frameworks to Anchor Single Ru Sites as Chemoselective Catalysts toward the Hydrogenation of Quinoline. Journal of the American Chemical Society, 2017, 139, 9419-9422.	13.7	558
219	Numerical simulation of the behavior of highâ€viscosity fluids falling film flow down the vertical wavy wall. Asia-Pacific Journal of Chemical Engineering, 2017, 12, 97-109.	1.5	6
220	Carbon-Based Oxamate Cobalt(III) Complexes as Bioenzyme Mimics for Contaminant Elimination in High Backgrounds of Complicated Constituents. Materials, 2017, 10, 1169.	2.9	5
221	Insights into the generation of high-valent copper-oxo species in ligand-modulated catalytic system for oxidizing organic pollutants. Chemical Engineering Journal, 2016, 304, 1000-1008.	12.7	18
222	The coupling of hemin with persistent free radicals induces a nonradical mechanism for oxidation of pollutants. Chemical Communications, 2016, 52, 9566-9569.	4.1	30
223	Self-floating graphitic carbon nitride/zinc phthalocyanine nanofibers for photocatalytic degradation of contaminants. Journal of Hazardous Materials, 2016, 317, 17-26.	12.4	64
224	Electrocatalytic degradation of organic contaminants using carbon fiber coupled with cobalt phthalocyanine electrode. Journal of Applied Electrochemistry, 2016, 46, 583-592.	2.9	19
225	Graphitic Carbon Nitride from Burial to Re-emergence on Polyethylene Terephthalate Nanofibers as an Easily Recycled Photocatalyst for Degrading Antibiotics under Solar Irradiation. ACS Applied Materials & Interfaces, 2016, 8, 25962-25970.	8.0	56
226	Atomically Dispersed Ru on Ultrathin Pd Nanoribbons. Journal of the American Chemical Society, 2016, 138, 13850-13853.	13.7	132
227	Electrodeposition of polypyrrole on carbon nanotube-coated cotton fabrics for all-solid flexible supercapacitor electrodes. RSC Advances, 2016, 6, 13359-13364.	3.6	51
228	Catalytic degradation of recalcitrant pollutants by Fenton-like process using polyacrylonitrile-supported iron (II) phthalocyanine nanofibers: Intermediates and pathway. Water Research, 2016, 93, 296-305.	11.3	106
229	The consortium of heterogeneous cobalt phthalocyanine catalyst and bicarbonate ion as a novel platform for contaminants elimination based on peroxymonosulfate activation. Journal of Hazardous Materials, 2016, 301, 214-221.	12.4	66
230	Key role of activated carbon fibers in enhanced decomposition of pollutants using heterogeneous cobalt/peroxymonosulfate system. Journal of Chemical Technology and Biotechnology, 2016, 91, 1257-1265.	3.2	44
231	Cube-like Cu2MoS4 photocatalysts for visible light-driven degradation of methyl orange. AIP Advances, 2015, 5, 077130.	1.3	22
232	Enhanced catalytic decoloration of Rhodamine B based on 4â€aminopyridine iron coupled with cellulose fibers. Journal of Chemical Technology and Biotechnology, 2015, 90, 1144-1151.	3.2	10
233	Interfacial peroxidase-like catalytic activity of surface-immobilized cobalt phthalocyanine on multiwall carbon nanotubes. RSC Advances, 2015, 5, 9374-9380.	3.6	30
234	Visible-light responsive electrospun nanofibers based on polyacrylonitrile-dispersed graphitic carbon nitride. RSC Advances, 2015, 5, 86505-86512.	3.6	32

#	Article	IF	CITATIONS
235	Raman scattering of single crystal Cu2MoS4 nanosheet. AIP Advances, 2015, 5, 037141.	1.3	25
236	Self-assembly of ultrathin Cu ₂ MoS ₄ nanobelts for highly efficient visible light-driven degradation of methyl orange. Nanoscale, 2015, 7, 17998-18003.	5.6	36
237	Oxidative desulfurization of dibenzothiophene with molecular oxygen catalyzed by carbon fiber-supported iron phthalocyanine. Reaction Kinetics, Mechanisms and Catalysis, 2014, 111, 535-547.	1.7	32
238	Enhanced removal of acid red 1 with large amounts of dyeing auxiliaries: the pivotal role of cellulose support. Cellulose, 2014, 21, 2073-2087.	4.9	6
239	Solvothermal Synthesis of Ternary Cu ₂ MoS ₄ Nanosheets: Structural Characterization at the Atomic Level. Small, 2014, 10, 4637-4644.	10.0	97
240	Effects of physical aging on the selfâ€healing, shape memory, and crystallization behaviors of hydrogenâ€bonded supramolecular polymers. Journal of Polymer Science, 0, , .	3.8	0
241	Constructing the separation pathway for photo-generated carriers by diatomic sites decorated on MIL-53-NH2(Al) for enhanced photocatalytic performance. Nano Research, 0, , .	10.4	8